The human NKG2D ligand ULBP2 can be expressed at the cell surface with or without a GPI anchor and both forms can activate NK cells

Lola Fernández-Messina[1], Omodele Ashiru[1], Sonia Agüera-González[1], Hugh T. Reyburn[2] and Mar Valés-Gómez[1,2,*]

[1]Department of Pathology, University of Cambridge, Tennis Court Road, Cambridge CB2 1QP, UK
[2]Centro Nacional de Biotecnología, Darwin 3, Campus de Cantoblanco, E-28049 Madrid, Spain
*Author for correspondence (mvales@cnb.csic.es)

Accepted 6 October 2010
Journal of Cell Science 124, 321-327

doi:10.1242/jcs.076042

Summary

The activating immune receptor NKG2D binds to several stress-induced ligands that are structurally different. MHC-class-I-related chain (MIC) A/B molecules have a transmembrane domain, whereas most UL16 binding proteins (ULBPs) are glycosylphosphatidylinositol (GPI)-linked molecules. The significance of this variability in membrane anchors is unclear. Here, we demonstrate that ULBP2, but not ULBP1 or ULBP3, can reach the cell surface without the GPI modification. Several proteins are expressed at the cell surface as both transmembrane and GPI-linked molecules, either via alternative splicing or by the expression of linked genes. However, to our knowledge, ULBP2 is the first single mammalian cDNA that can be expressed as either a transmembrane or a GPI-anchored protein. The rate of maturation and the levels of cell surface expression of the non-GPI-linked form were lower than those of the GPI-linked ULBP2. Nonetheless, non-GPI ULBP2 was recognised by NKG2D and triggered NK cell cytotoxicity. These data show that differences in membrane attachment by NKG2D ligands are more important for regulation of their surface expression than for cytotoxic recognition by NKG2D and emphasise that detailed characterisation of the cell biology of individual NKG2D ligands will be necessary to allow targeted modulation of this system.

Key words: GPI-anchored proteins, NKG2D, Innate immunity, Detergent-resistant membranes, ER trafficking

Introduction

NKG2D is a C-type lectin-like receptor that can stimulate both cytotoxicity and cytokine secretion by NK cells, TCR$\gamma\delta^+$ and $CD8^+$ TCR$\alpha\beta^+$ T cells (for reviews, see Lopez-Larrea et al., 2008; Nausch and Cerwenka, 2008). Receptor ligation can costimulate the activation of naive T cells (Maasho et al., 2005) and can even trigger cytotoxicity by IL-2-activated T cells in the absence of TCR ligation (Verneris et al., 2004). The ligands for NKG2D are related to MHC class I molecules, but unlike these proteins, the expression of NKG2D ligands is restricted or absent on normal tissues, instead they are upregulated in situations of stress and disease such as pathogen infection or tumour transformation to render these cells susceptible to NK cell lysis (Gonzalez et al., 2006). In humans, eight ligands of NKG2D have been identified, which are members of either the MIC (MICA and MICB) (Bahram et al., 1994; Bahram et al., 1996) or the ULBP (ULBP1, ULBP2, ULBP3, ULBP4, RAET1G and RAET1L) family (Chalupny et al., 2003; Cosman et al., 2001; Eagle et al., 2009). The biological significance of the existence of multiple ligands for one receptor is poorly understood, but might reflect differences in the biochemistry and cell biology of the different ligands, which lead to differential roles for these molecules in immune surveillance as an evolutionary response to selective pressures exerted by pathogens or cancer. Consistent with this hypothesis NKG2D ligands are variable in both their amino acid sequence and domain structure. All ligands share an MHC class-I-like $\alpha1$–$\alpha2$ domain that binds to NKG2D, but whereas the MICA/B proteins have an MHC-class-I-like $\alpha3$ domain, ULBP1–ULBP3 and ULBP6 (RAET1L) are anchored to the membrane through a glycosylphosphatidylinositol (GPI) moiety. ULBP4 (also known as RAET1E) and ULBP5 (RAET1G) proteins also have transmembrane domains and cytoplasmic tails of variable length and sequence. However, the functional significance of these extensive structural differences between NKG2D ligands for immune activation is not clear. In particular, the significance of the presence of a GPI anchor in some NKG2D ligands, whereas others contain transmembrane and cytoplasmic domains, is unknown. In the mouse, GPI-anchored proteins have modest to low affinities for NKG2D, whereas the ligands possessing transmembrane and cytoplasmic domains have high affinity (O'Callaghan et al., 2001), but it is not known whether the human NKG2D ligands conform to this pattern. In any case, differences in cellular distribution between GPI-anchored and transmembrane (TM) proteins might also affect the strength of the receptor–ligand interaction because GPI-anchored proteins tend to be found in localised regions of the membrane that are rich in sphingolipids and cholesterol, known as lipid rafts (Sharom and Lehto, 2002). Clustering of the GPI-anchored ULBPs within lipid rafts, which are known to polarise to the site of the interaction of an NK cell with a susceptible target cell (Lou et al., 2000), might increase the avidity of their interaction with the NKG2D receptor.

Another possible relevant difference between GPI-anchored and TM proteins is that within polarised epithelial layers, GPI-anchored proteins have a greater tendency to be found at the apical surface

Journal of Cell Science

(Paulick and Bertozzi, 2008), whereas TM proteins are often targeted to the basal or lateral sides of the cell. Normal wild-type (wt) MICA is targeted to the basolateral membrane of gut epithelium, in proximity to NK or T cells, where it can signal cell destruction. However, a naturally occurring allele that has a TM motif, but no cytoplasmic tail, is found instead at the apical surface, where there is a greater concentration of lipid rafts and less contact with NKG2D-bearing cells (Suemizu et al., 2002). Thus the differences in anchorage of NKG2D ligands could be associated with differential distribution of these molecules in the same cell and differential availability to lymphocytes.

We have shown differences in the shedding mechanisms of different ULBP molecules (Fernandez-Messina et al., 2010) and now provide evidence to demonstrate that the NKG2D ligand ULBP2, and not the other GPI-anchored ULBPs, although it is principally expressed at the cell surface as a GPI-linked molecule, can reach the cell surface without this modification. The transmembrane form of ULBP2 is expressed at lower levels than the GPI form; however, its ability to stimulate NKG2D-dependent NK-cell-mediated cytotoxicity is maintained.

Results

ULBP2 is expressed on the cell surface in the absence of a GPI moiety

The sequence of the ULBP family of NKG2D ligands predicted that ULBP1–ULBP3 would be expressed on the cell surface as GPI-anchored proteins. However, the first description of the ULBPs showed that although expression levels of ULBP1 and ULBP3 were reduced about 50% after treatment with phosphatidylinositol-specific phospholipase C (PI-PLC), PI-PLC treatment only reduced cell surface expression of ULBP2 by around 30% (Cosman et al., 2001). These data prompted us to re-evaluate the GPI linkage of the ULBP proteins, and for this purpose we used a genetic system: transfection of CHO cells (parental CHO G9PLAP, referred to as CHO) and mutagenised CHO cells (CHO G9PLAP.85, referred to as CHO ΔGPI) that were unable to synthesise GPI anchors because of a deficiency in PIG-L, a key enzyme in the second step of biosynthesis of GPI anchors. Initially, to avoid artefacts associated with the selection of particular clones during the generation of stable transfectants, these experiments were done by transiently transfecting parental CHO and CHO ΔGPI cells with expression constructs encoding ULBP1, ULBP2, ULBP3 and the transmembrane molecule MICB. As expected, the expression of MICB, a protein attached to the plasma membrane through a transmembrane region, was comparable between the parental and mutant cell lines. Strikingly, however, although ULBP1 and ULBP3 were not expressed on the cell surface of the GPI-deficient CHO cells, significant levels of ULBP2 were detected by FACS analysis (Fig. 1A). In control experiments, western blot analysis of cell lysates prepared from the transiently transfected cells demonstrated expression of the ULBP1, ULBP2 and ULBP3 proteins in both the wt and ΔGPI CHO transfectants (Fig. 1B). The different bands observed on comparison of the CHO and CHO ΔGPI lysates presumably reflect the presence of unmodified and GPI-modified ULBP proteins in variable proportions. The presence of intracellular ULBP1 and ULBP3 and their absence from the cell surface, was confirmed by flow cytometry after fixation, permeabilisation and intracellular staining (data not shown). These data strongly suggest that ULBP1 and ULBP3 are modified by the addition of a GPI moiety for surface expression, confirming that these molecules are preferentially expressed as GPI-linked proteins. By contrast,

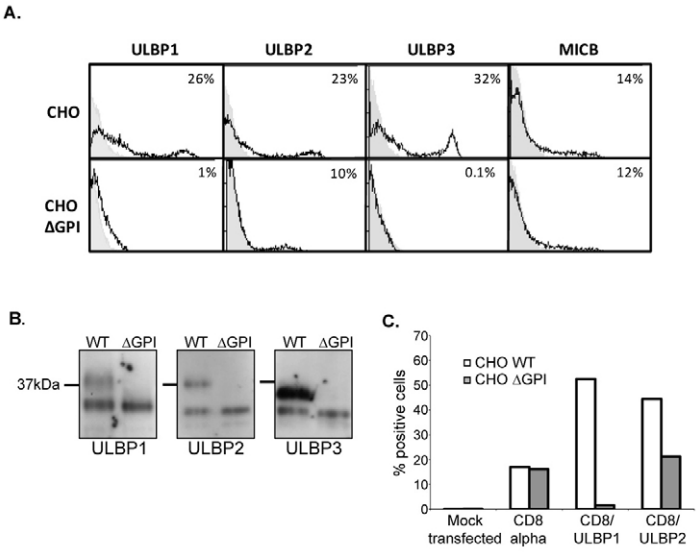

Fig. 1. ULBP2 can be expressed at the cell surface in the absence of GPI machinery in transient transfectants. Parental CHO and the GPI-deficient mutant CHO cell line (ΔGPI) were transiently transfected with ULBP1, ULBP2, ULBP3 and MICB and analysed by (**A**) flow cytometry and (**B**) western blot. Grey: isotype control; black line: ULBP or MIC staining. The same cell lines were also transiently transfected with CD8 and chimeric molecules containing the extracellular region of CD8 and the C-terminal region of the indicated ULBPs (as in supplementary material Fig. S1). (**C**) The percentage of positive cells assessed by flow cytometry.

although the levels of surface expression of ULBP2 were higher in the CHO cells than in the ΔGPI cell line, some ULBP2 was expressed at the surface of these cells suggesting that modification by addition of GPI moieties is not an absolute requirement for surface expression of ULBP2 and that the transmembrane sequence present in the C-terminal portion of full-length ULBP2 might be competent for expression at the plasma membrane. To explore this hypothesis further, chimaeras comprising the extracellular domain of CD8α and the C-terminus of either ULBP1 or ULBP2, including the predicted site of GPI modification were constructed (supplementary material Fig. S1). Transient transfection of the wt CHO and CHO ΔGPI-deficient cells with the chimaeric proteins confirmed that the CD8–ULBP2 chimaera could be expressed at the cell surface whereas the CD8–ULBP1 chimaera was not (Fig. 1C). These data demonstrate that the ability of ULBP2 to localise to the plasma membrane in the absence of a GPI anchor is determined by the C-terminal region, where the signal for the attachment of the anchor is located.

The observation that ULBP2 could be expressed on the cell surface of a cell line unable to synthesise GPI anchors was surprising, because it is thought that there is a tight correlation between the attachment of the GPI anchor and the ability of the GPI-anchored protein to progress from the ER to the Golgi (Moran et al., 1991). On translation, GPI-linked proteins are inserted in the ER membrane through a C-terminal hydrophobic region located after the GPI anchor signal site. These transmembrane proteins are then cleaved and a pre-assembled GPI moiety is attached to the so-called ω residue through the action of a multi-enzyme complex. The lack of an essential enzyme required for GPI anchor synthesis results in a non-cleaved protein precursor that still contains a hydrophobic region, but shorter than a typical transmembrane

domain, which is believed to lead to the precursor being recognised and retained by the quality-control system of the ER (Mayor and Riezman, 2004). In this light it was important to rigorously confirm that the ULBP2 protein expressed in the CHO ΔGPI cells was not GPI anchored and that it could still reach the cell surface. For this purpose, stable transfectants in CHO and CHO ΔGPI cells were produced (Fig. 2A). Consistent with the data from the transient transfection experiments, ΔGPI-deficient cells expressed ULBP2 at a lower level than observed in wt CHO cells. As shown in supplementary material Fig. S2A, the proportion of mature and immature ULBP2 varied between the two cell lines: in wt cells, the majority of the expressed ULBP2 was in the upper band, corresponding to mature protein, whereas in GPI-deficient cells, ULBP2 was mainly immature and migrated faster in SDS-PAGE.

To analyse the presence of ULBP2 at the plasma membrane, surface proteins were labelled using sulfo-NHS-biotin, which is unable to cross the plasma membrane. Total ULBP2 was immunoprecipitated and surface protein was analysed by western blot using streptavidin–HRP (Fig. 2B). Control immunoprecipitations of actin demonstrated that the biotin labelling was cell surface specific because no actin was visible when the western was probed with streptavidin (Fig. 2B, left), but actin protein was detected when probing with anti-actin antibody (Fig. 2B, right). In these experiments, Endoglycosidase H (EndoH) was used to discriminate between proteins that are still in the ER (sensitive to EndoH digestion) and those that have progressed further through the secretory pathway. As expected, cell surface mature protein was resistant to EndoH cleavage. In total lysates, only the intracellular lower band was susceptible to cleavage by EndoH (supplementary material Fig. S2B). These data confirmed the presence of ULBP2 at the cell surface of cells deficient for GPI synthesis.

To test for the presence of a GPI anchor, ULBP2-transfected CHO and CHO ΔGPI cells were treated with bacterial PI-PLC. Loss of ULBP2 from the membrane and its appearance in the supernatant was assayed, after incubation with PI-PLC, by using temperature-induced phase separation of Triton X-114 (Bordier, 1981). After incubation at 37°C, Triton X-114 separates in two phases: the lower, detergent-rich phase, where membrane-bound proteins are found; and the upper, aqueous phase, where soluble hydrophilic proteins are recovered. In these experiments, membrane bound GPI-anchored proteins are expected in the detergent phase and, after digestion with PI-PLC, cleaved hydrophilic proteins move to the aqueous phase. These data (Fig. 2C) confirmed that although ULBP2 expressed in CHO cells was highly susceptible to cleavage with PI-PLC, the ULBP2 found in CHO ΔGPI cells was essentially unaffected by treatment with this enzyme.

The presence of ULBP2 as a non-GPI-linked protein in transfectants was not an artefact of the transfection system, because these data could be reproduced in a mutagenised K562 cell line defective in GPI anchor (Mohney et al., 1994) that expressed ULBP1 and ULBP2 endogenously. Indeed, although ULBP1 was unable to reach the cell surface in the mutant cell line, ULBP2 was still present at the plasma membrane (Fig. 3). This result was not due to the absence of ULBP1 in the GPI-deficient cell line because it was possible to detect intracellular protein after staining of permeabilised cells.

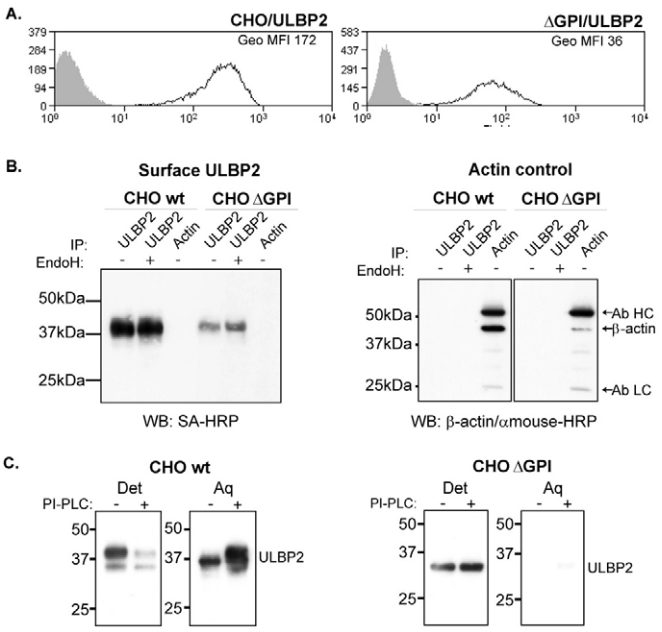

Fig. 2. ULBP2 can be expressed at the cell surface in the absence of GPI machinery in stable transfectants. (**A**) Flow cytometry showing cell surface expression of ULBP2 stably transfected in parental CHO and in the GPI-deficient CHO cell line. (**B**) Cell surface proteins were labelled by biotinylation. ULBP2 was immunoprecipitated and, after SDS-PAGE and western transfer, visualised with streptavidin-peroxidase and ECL. As a control for the cell-surface specificity of biotinylation, β-actin was also immunoprecipitated. No β-actin could be detected after probing with streptavidin–HRP (left), however actin protein was detected when the blot was probed with actin-specific monoclonal antibody (right), demonstrating that the actin immunoprecipitation has worked correctly, but that only cell surface proteins are biotinylated. (**C**) CHO and GPI-deficient cells transfected with ULBP2 were treated with the enzyme PI-PLC to remove GPI-anchored proteins from the cell surface. After digestion, cells were lysed in Triton X-114 and membrane and soluble proteins were fractionated. The resulting detergent (membrane) and aqueous (soluble) fractions were analysed by western blot with ULBP2 specific polyclonal antibodies.

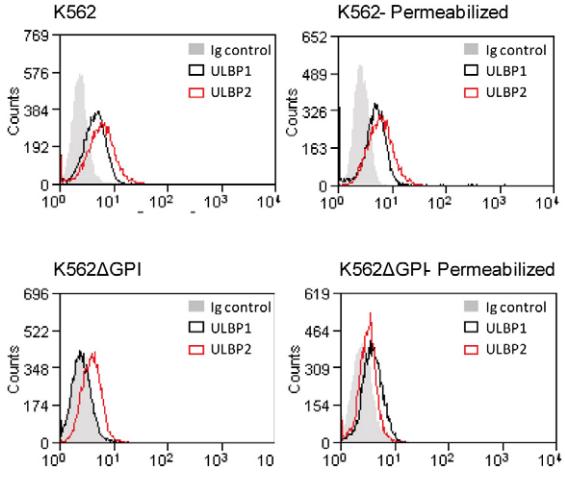

Fig. 3. Endogenous ULBP2, but not ULBP1, is expressed at the surface of GPI-deficient K562 cells. K562 cells and K562 class K mutants were stained with monoclonal antibodies specific for ULBP1, ULBP2 and an isotype control and analysed by flow cytometry. ULBP1 and ULBP2 are expressed in the cell, as shown by intracellular staining, but only ULBP2 appears at the cell surface of GPI-deficient cells.

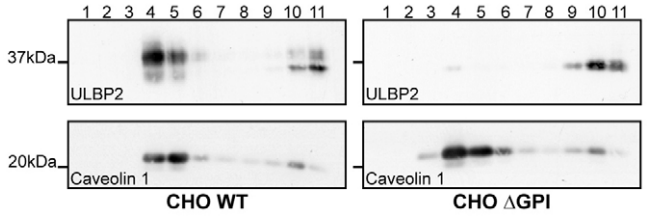

Fig. 4. The majority of ULBP2 is present in detergent-resistant membranes of wild-type, but not GPI-deficient CHO cell lines. CHO cells and ΔGPI cells transfected with ULBP2 were lysed and fractionated by centrifugation on discontinuous sucrose gradients. Equal volumes of these fractions were analysed by western blot for the presence of ULBP2. As a positive control for fractionation, the presence of caveolin-1 in the different fractions was also analysed.

Transmembrane ULBP2 is poorly recruited to detergent-resistant membranes

Proteins with a GPI moiety are usually recruited to domains of the membrane that are rich in cholesterol and sphingolipids and are unable to be solubilised in the presence of detergents such as Brij58 and Triton X-100. ULBP3 has been shown to be included in lipid rafts (Eleme et al., 2004); however, no data are available on ULBP2. As predicted, ULBP2 was recruited to lipid rafts in parental CHO cells, but excluded from the microdomains when the protein was expressed in GPI-deficient cells (Fig. 4). It is interesting to note that the size of the majority of the protein in ΔGPI cells is apparently smaller than that seen in CHO cells, again reflecting that the more abundant biochemical species are different in the two cell lines.

Maturation of ULBP2

The modification of proteins by attachment of a GPI moiety is tightly regulated by the ER quality control machinery. Thus, it was of interest to analyse the ability of ULBP2 to progress in the secretory pathway in the presence and absence of the GPI anchor. Interestingly, pulse-chase experiments showed that wt ULBP2 progressed through the secretory pathway more slowly than ULBP3: whereas ULBP3 rapidly acquired resistance to EndoH digestion, almost 30% of ULBP2 was still immature even after 180 minutes of chase (Fig. 5A). Consistent with these data, confocal microscopy showed the presence of significant amounts of intracellular protein (Fig. 5B). These observations suggest that either the folding or the GPI modification occurs significantly more slowly for ULBP2 than for ULBP3. The absence of the GPI synthesis machinery slowed the rate of maturation of ULBP2 even more dramatically (Fig. 5C). Most of the protein was immature (Fig. 5C) and intracellular (Fig. 5B), suggesting that the reduced levels of ULBP2 cell surface expression observed in the GPI-deficient cell line reflect the low efficiency of exit of non-GPI linked ULBP2 from the ER. The percentages of mature and immature protein in the two cell lines are summarised in Fig. 5D.

Non-GPI linked ULBP2 is recognised by NKG2D

The contribution of the GPI anchor to the functional activity of ULBP2 was explored next. First, the ability of the protein to be recognised by the NKG2D receptor was evaluated in flow cytometry experiments. NKG2D–Ig recombinant protein was used to stain the CHO and ΔGPI cell lines stably transfected with ULBP2 (Fig. 6A). Although, in these experiments the total amount of ULBP2 protein expressed at the surface of these transfectants was quite different, the value for half-maximal binding of the NKG2D–Ig was comparable in both cell lines, thus it seems reasonable to conclude that the affinity of the receptor–ligand interaction was similar in both instances.

The recognition of GPI-deficient ULBP2 was then analysed in cytotoxicity assays (Fig. 6B). The absence of a GPI anchor did not appreciably affect the recognition by NK cells, suggesting that although differences in the form of membrane anchor of the ULBP2 molecule might be associated with differences in their responses to

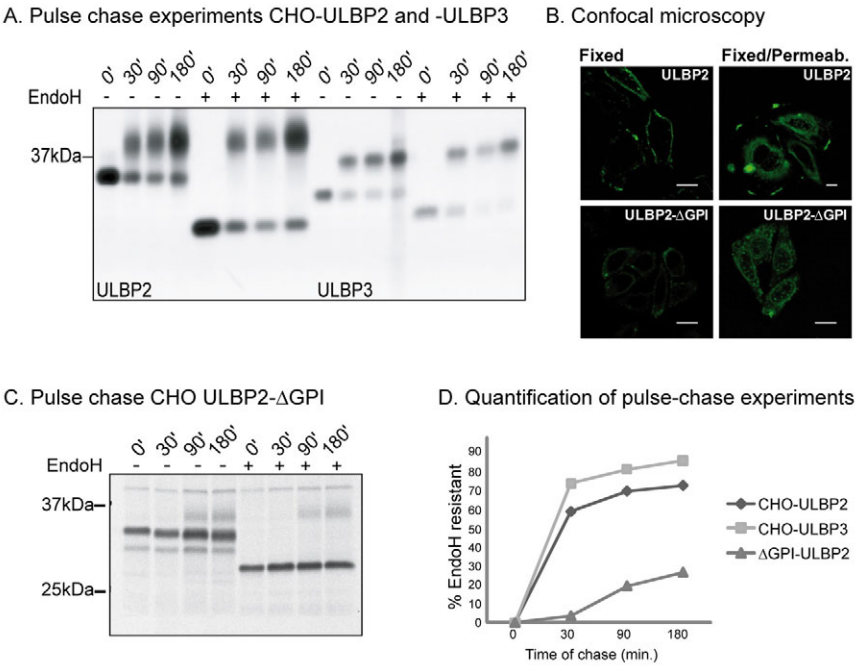

Fig. 5. ULBP2 matures more slowly than ULBP3 in parental CHO cells and, in GPI-deficient cells, the rate of egress of ULBP2 from the ER is still slower. (**A**) Stable transfectants of ULBP2 and ULBP3 were metabolically labelled with [^{35}S]Met/Cys for 10 minutes and chased for the indicated times. Lysates were prepared and the ULBP molecules immunoprecipitated; one half of the immunoprecipitated material was digested with EndoH before being analysed by SDS-PAGE. (**B**) CHO and ΔGPI cells transfected with ULBP2 were cultured on coverslips, fixed, or fixed and permeabilised (as indicated) and stained with polyclonal antibody specific for ULBP2. Scale bar: 10 μm. (**C**) ΔGPI cells stably transfected with ULBP2 were pulse-labelled with [^{35}S]Met/Cys and chased for the indicated times before immunoprecipitation, digestion with EndoH and analysis by SDS-PAGE. (**D**) Quantification of mature vs immature ULBPs. The percentage of mature protein present in each one of the bands of the experiments shown in A and C was analysed using Image J.

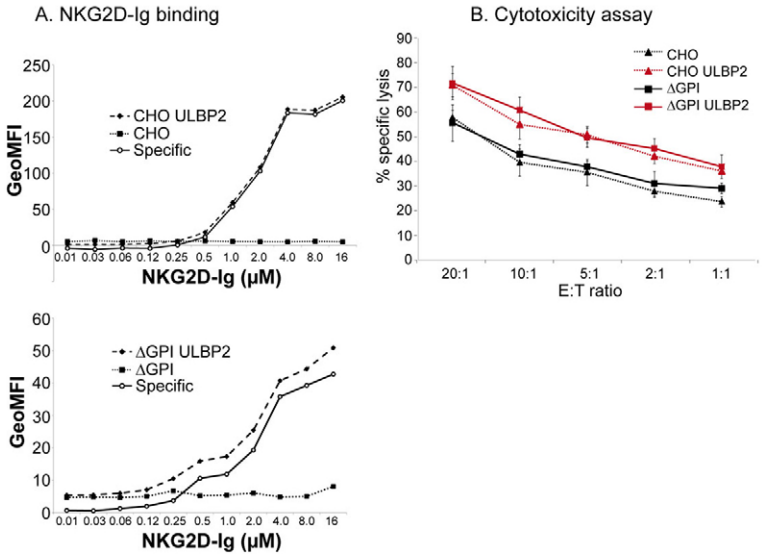

Fig. 6. ULBP2 molecules expressed in either the CHO wild-type or GPI-deficient cells interact similarly with NKG2D. (**A**) Increasing amounts of recombinant human NKG2D–Ig fusion protein were used to stain untransfected and ULBP2-transfected CHO and ΔGPI cells. Specific staining was calculated by subtracting the mean fluorescence intensity (MFI) of NKG2D staining of the untransfected cells from the MFI of NKG2D staining of the ULBP2 transfectant. One representative experiment of three is shown. (**B**) Primary NK cells were used as effectors in a cytotoxicity assay to assess the susceptibility of the untransfected and ULBP2 transfected CHO and ΔGPI cells to lysis. The data shown are the mean ± s.d. values for % specific cytotoxicity from three experiments.

stress pathways, once at the cell surface, both forms of ULBP2 are equally competent to trigger cytolysis by NK cells. In support of these data, wt CHO and CHO ΔGPI cells expressing ULBP2 were equally able to stimulate NK cell degranulation in experiments measuring the appearance of LAMP1 at the plasma membrane after exposure to target cells for 2 hours (data not shown).

Discussion

In summary, the data presented here reveal that although the NKG2D ligand ULBP2 is normally expressed as a GPI-linked molecule, it can reach the cell surface without undergoing this modification; however, in these circumstances, the level of cell surface expression is lower. Although other proteins can also be expressed at the cell surface as both transmembrane and GPI-anchored molecules, they achieve this duality either as a result of alternative splicing, as for example with CD58 (Dustin and Springer, 1991), or by expression from closely linked genes that encode either a transmembrane form or a GPI-linked form, as with CD16 (Ravetch and Perussia, 1989). By contrast, our data show that a single cDNA clone of ULBP2 can be expressed at the cell surface in either a transmembrane or GPI-linked form. The data with CD8–ULBP2 chimaeras clearly show that the ability of ULBP2 to be present at the plasma membrane in the absence of a GPI anchor is determined by the C-terminal amino acids of ULBP2, but mutagenesis studies will be required to further characterise this phenomenon. Functionally, the data show that both GPI-linked and transmembrane ULBP2, despite marked differences in levels of cell surface expression are equally able to stimulate NK cell cytotoxicity. The ligation of the NKG2D receptor by ligand is known to be a particularly potent stimulus to activate NK cell killing (Cosman et al., 2001) and this probably explains why the approximately fivefold difference in cell surface expression does not lead to a significant difference in susceptibility of the CHO ULBP2 and ΔGPI ULBP2 cells to NK lysis. These data suggest either that GPI-anchored and transmembrane versions of the ULBP2 protein have equal lateral mobility in the membrane, or else that increased lateral mobility is not advantageous for this molecule in stimulating NK cytotoxic function.

The biological significance of the existence of multiple ligands for NKG2D is a recurrent question in the field and it has been proposed that it might reflect differences in the biochemistry and cell biology of the different ligands that have evolved in response to selective pressures exerted by pathogens or cancer. We have demonstrated previously that the different NKG2D ligands are released from cells by different routes and these new data demonstrate that individual ULBPs have different trafficking rates through the secretory pathway and that the regulation of their surface expression depends on the C-terminal region of the protein. The fact that ULBP2 can reach the cell surface even in the absence of the complete machinery for synthesis of GPI anchors supports the idea that different stress stimuli might affect the various ULBPs in different manners. In particular, our data suggest that although ULBP2 is normally expressed as a GPI-linked molecule, it can reach the cell surface as a transmembrane protein where it can activate NKG2D-dependent cytotoxicity by NK cells. Thus, although this alternative pathway for expression of ULBP2 is rarely used, ULBP2 expression could still be induced for immune surveillance, even after stresses or mutations that reduce or block GPI anchor synthesis (see model in supplementary material Fig. S3).

It is interesting to note that upregulation of NKG2D ligands in cancer has been associated with very different outcomes for different types of cancer. For example, high tumour expression of MIC and/or ULBPs was associated with improved patient survival in colorectal cancer (McGilvray et al., 2009), whereas in ovarian cancer, high expression of several NKG2D ligands was inversely correlated with patient survival (McGilvray et al., 2010). Analysis of the NKG2D system in disease is complex because of the large number of distinct ligands for a single receptor and the possibility of regulation by released soluble ligands. Our work shows that there are significant differences in the cell biology of these various ligand molecules and that further study is needed to understand how the different stress situations affect the upregulation, release and function of the different NKG2D ligands and how these factors impact immune responses towards different types of cancer.

Materials and Methods

Cells and reagents

ULBP1, ULBP2 and ULBP3 constructs were obtained from Richard Apps (Apps et al., 2008). Chinese Hamster Ovary (CHO) G9PLAP cells and the GPI-deficient mutant CHO G9PLAP.85 (referred as CHO ΔGPI) (Stevens et al., 1996) (kind gifts from Victoria L. Stevens, American Cancer Society, Atlanta, GA and Saulius Vainauskas, Medical College of Cornell University, NY) were maintained in Hams F12 medium with supplements. CHO cells were transfected, using Lipofectamine

2000 (Invitrogen), with a mixture (9:1 ratio) of each ULBP expression plasmid with a vector conferring resistance to puromycin for stable transfectants (de la Luna and Ortin, 1992). Stable transfectants were sorted where necessary and grown in selective medium (8 μg/ml puromycin, Calbiochem). The isolation and culture of human primary polyclonal NK cells was as previously described (Ashiru et al., 2010). K562 class K mutants (a kind gift from M. Edward Medof, Case Western Reserve University, Cleveland, OH) were maintained in RPMI with 10% FCS (Mohney et al., 1994; Yu et al., 1997). Antibodies directed against ULBPs were purchased from R&D systems (Abingdon, UK) and the anti-KDEL antibody was from StressGen. B9.4 antibody directed against CD8 was a gift from Jack L. Strominger (Harvard University, Cambridge, MA). Leupeptin, Pepstatin A, 1-10 phenanthroline, PI-PLC were purchased from Sigma. NKG2D–Ig fusion protein was prepared as previously described (Vales-Gomez et al., 2003).

Flow cytometry

10^5 cells were preincubated in PBS containing 1% bovine serum albumin, 0.1% sodium azide (PBA). Cells were then incubated with mouse monoclonal antibodies and bound antibody was visualised using either phycoerythrin- or FITC-labelled $F(ab')_2$ fragments of goat anti-mouse Ig (Dako). For staining with the NKG2D–Ig fusion protein, bound protein was visualised using PE-labelled anti-human Ig (Immunotech). Samples were analysed using a FACScan II flow cytometer (Becton Dickinson). Dead cells were excluded from all analyses by staining with propidium iodide.

Intracellular staining was performed by permeabilisation using saponin: cells were fixed using 1% paraformaldehyde for 20 minutes at 4°C, washed twice with PBS containing 0.1% saponin and 1% BSA and incubated with for 10 minutes at room temperature. Cells were then washed and stained as usual using PBA buffer containing 0.1% saponin.

Western blot

Cell lysates were prepared by incubation in TNE buffer containing 1% NP-40 and the protease inhibitors leupeptin, pepstatin and 1,10 phenanthroline, for 30 minutes at 4°C. Nuclei were eliminated by centrifugation at 13,000 ***g***. Lysates and membrane-soluble fractionations were run on 12% SDS-PAGE gels and transferred to Immobilon-P (Millipore) membrane. The membrane was blocked using PBS containing 0.1% Tween-20 (PBS-T) and 5% non-fat dry milk. Detection of ULBP was performed by incubation with biotinylated goat polyclonal anti-ULBP antibody, followed by horseradish peroxidase-conjugated streptavidin. Proteins were visualised using the ECL system (Amersham Pharmacia). In some experiments, samples were treated with Endoglycosidase H (EndoH) (New England Biolabs, Ipswich, MA), according to the manufacturer's instructions.

Preparation of CD8–ULBP chimaeras

The C-terminal portions of ULBP1 and ULBP2 were amplified by PCR using the oligonucleotides: ULBP1for, 5′-GCATACAGCTGGATCCAACAAAACCACC-3′; ULBP1rev, 5′-CGGAATTCATCTGCCAGCTAGAATGAAGC-3′; ULBP2for, 5′-CATACAGCTGGAGCCAAGTGCAGGAG-3′ and ULBP2rev, 5′-CGGAATTC-AGATGCCAGGGAGGATGAAGC-3′. The PCR products were then digested with *Pvu*II and *Eco*RI. The CD8–ULBP chimaeras were prepared in a three-way ligation with pCDNA3 digested with *Eco*RI and *Hin*dIII, the extracellular domain of CD8 as a *Hin*dIII–*Eco*RV fragment and the C-terminal portion of either ULBP1 or ULBP2 as *Pvu*II–*Eco*RI fragments. All plasmids were sequenced to verify the integrity of the constructs (supplementary material Fig. S1).

Triton X-114 fractionation

A 12% solution (w/v) of Triton X-114 was preconcentrated separating three times the aqueous and detergent phases by incubation at 30–37°C followed by centrifugation at 1000 ***g*** for 5 minutes. The resulting detergent was used as the stock of Triton X-114 for experiments. Cells were lysed in 1% Triton X-114 in TBS with protease inhibitors. Extraction was performed for 1 hour at 4°C, rotating. After removing insoluble debris by centrifugation at 13,000 ***g*** at 4°C, phases were separated by incubating at 37°C for 5 minutes and centrifugation at 300 ***g*** and 25°C. The upper aqueous phase and the lower detergent phase were analysed separately by western blot after trichloroacetic acid (TCA) precipitation.

DRM fractionation

Detergent-resistant and detergent-soluble membrane fractions were prepared as previously described (Boutet et al., 2009). Western blot was performed using antibodies specific for ULBP2 and caveolin, as control for the fractionation.

^{35}S pulse-chase experiments

40×10^6 CHO cells transfected with ULBP2 were harvested and starved for 30 minutes in 2 ml Met/Cys-free medium. Cells were then incubated in 2 ml of Met/Cys-free medium containing 1 mCi [^{35}S]methionine for 10 minutes and chased for intervals of 0, 30, 90, 180 minutes by addition of medium supplemented with 10% FCS as source of non-radioactive methionine. Cell lysates were prepared in 1% NP-40 lysis buffer. After preclearing the lysate with Pansorbin (Calbiochem), ULBP proteins were recovered by immunoprecipitation using goat polyclonal antibodies (R&D). Immunoprecipitated proteins were recovered using Protein G beads (GE Healthcare), washed three times in lysis buffer and digested with Endoglycosidase H (NEB), following the manufacturer's instructions. Proteins were resolved by 12% SDS-PAGE. Two independent experiments were performed.

Confocal microscopy

Cells were fixed with 4% paraformaldehyde at 4°C for 15 minutes or fixed and permeabilised by incubation with 0.1% saponin at room temperature for 10 minutes after fixation. The different preparations were stained with polyclonal anti-ULBP antibodies (R&D) and analysed by confocal microscopy as previously described (Aguera-Gonzalez et al., 2009). Fluorescence images were obtained using confocal microscopes (either Leica TCS-NT-UV confocal laser scanning microscope; Olympus IX81or Zeiss LSM510-Confocor 2). Images of fixed cells were taken using a 63× 1.32 NA objective with the confocal pinhole set to 1 Airy unit. Images were obtained by scanning series of single focal planes across the cell using either Leica TCS software, FV10-ASW1.7 or LSM5 Image Examiner. To explore the whole intracellular area, series of sections (total interval z=2–4 μm) were acquired.

Cytotoxicity assays

Cytotoxicity assays were carried out using a one-step fluorimetric assay based on the use of AlamarBlue (Invitrogen) (Nociari et al., 1998). Effector cells alone, target cells alone and mixes of effectors and target cells at the indicated E:T ratios were incubated with AlamarBlue in 96 well flat-bottomed plates at 37°C in a humidified 5% CO_2 incubator overnight. Following the incubation, the fluorescence of the AlamarBlue was read on a Synergy HT plate reader (Biotek) with excitation at 530 nm and emission at 590 nm at 37°C. The percentage specific lysis was calculated as 100×{(AF of targets alone)–[(AF of mix)–(AF of effectors alone)]}/AF of targets alone, where AF=absolute fluorescence units.

The authors would like to thank Drs M. E. Medof, V. L. Stevens and S. Vainauskas for GPI-deficient cell lines; C. Gross and F. Colucci for critically reading the manuscript. This work was supported by the MRC (New Investigator Grant to M.V.-G.) and FIS (PS09/00181 and PI08/1701). O.A. was supported by the Leukaemia Research Fund and The Newton Trust. S.A.-G. was supported by Fundación Caja Madrid and Ibercaja. Deposited in PMC for release after 6 months.

Supplementary material available online at
http://jcs.biologists.org/cgi/content/full/124/3/321/DC1

References

Aguera-Gonzalez, S., Boutet, P., Reyburn, H. T. and Vales-Gomez, M. (2009). Brief residence at the plasma membrane of the MHC class I-related chain B is due to clathrin-mediated cholesterol-dependent endocytosis and shedding. *J. Immunol.* **182**, 4800-4808.

Apps, R., Gardner, L., Traherne, J., Male, V. and Moffett, A. (2008). Natural-killer cell ligands at the maternal-fetal interface: UL-16 binding proteins, MHC class-I chain related molecules, HLA-F and CD48. *Hum. Reprod.* **23**, 2535-2548.

Ashiru, O., Boutet, P., Fernandez-Messina, L., Aguera-Gonzalez, S., Skepper, J. N., Vales-Gomez, M. and Reyburn, H. T. (2010). Natural killer cell cytotoxicity is suppressed by exposure to the human NKG2D ligand MICA*008 that is shed by tumor cells in exosomes. *Cancer Res.* **70**, 481-489.

Bahram, S., Bresnahan, M., Geraghty, D. E. and Spies, T. (1994). A second lineage of mammalian major histocompatibility complex class I genes. *Proc. Natl. Acad. Sci. USA* **91**, 6259-6263.

Bahram, S., Mizuki, N., Inoko, H. and Spies, T. (1996). Nucleotide sequence of the human MHC class I MICA gene. *Immunogenetics* **44**, 80-81.

Bordier, C. (1981). Phase separation of integral membrane proteins in Triton X-114 solution. *J. Biol. Chem.* **256**, 1604-1607.

Boutet, P., Aguera-Gonzalez, S., Atkinson, S., Pennington, C. J., Edwards, D. R., Murphy, G., Reyburn, H. T. and Vales-Gomez, M. (2009). Cutting edge: the metalloproteinase ADAM17/TNF-alpha-converting enzyme regulates proteolytic shedding of the MHC class I-related chain B protein. *J. Immunol.* **182**, 49-53.

Chalupny, N. J., Sutherland, C. L., Lawrence, W. A., Rein-Weston, A. and Cosman, D. (2003). ULBP4 is a novel ligand for human NKG2D. *Biochem. Biophys. Res. Commun.* **305**, 129-135.

Cosman, D., Mullberg, J., Sutherland, C. L., Chin, W., Armitage, R., Fanslow, W., Kubin, M. and Chalupny, N. J. (2001). ULBPs, novel MHC class I-related molecules, bind to CMV glycoprotein UL16 and stimulate NK cytotoxicity through the NKG2D receptor. *Immunity* **14**, 123-133.

de la Luna, S. and Ortin, J. (1992). pac gene as efficient dominant marker and reporter gene in mammalian cells. *Methods Enzymol.* **216**, 376-385.

Dustin, M. L. and Springer, T. A. (1991). Role of lymphocyte adhesion receptors in transient interactions and cell locomotion. *Annu. Rev. Immunol.* **9**, 27-66.

Eagle, R. A., Traherne, J. A., Hair, J. R., Jafferji, I. and Trowsdale, J. (2009). ULBP6/RAET1L is an additional human NKG2D ligand. *Eur. J. Immunol.* **39**, 3207-3216.

Eleme, K., Taner, S. B., Onfelt, B., Collinson, L. M., McCann, F. E., Chalupny, N. J., Cosman, D., Hopkins, C., Magee, A. I. and Davis, D. M. (2004). Cell surface organization of stress-inducible proteins ULBP and MICA that stimulate human NK cells and T cells via NKG2D. *J. Exp. Med.* **199**, 1005-1010.

Fernandez-Messina, L., Ashiru, O., Boutet, P., Aguera-Gonzalez, S., Skepper, J. N., Reyburn, H. T. and Vales-Gomez, M. (2010). Differential mechanisms of shedding of the glycosyl-phosphatidylinositol (GPI)-anchored NKG2D ligands. *J. Biol. Chem*. **285**, 8543-8551.

Gonzalez, S., Groh, V. and Spies, T. (2006). Immunobiology of human NKG2D and its ligands. *Curr. Top. Microbiol. Immunol.* **298**, 121-138.

Lopez-Larrea, C., Suarez-Alvarez, B., Lopez-Soto, A., Lopez-Vazquez, A. and Gonzalez, S. (2008). The NKG2D receptor: sensing stressed cells. *Trends Mol. Med.* **14**, 179-189.

Lou, Z., Jevremovic, D., Billadeau, D. D. and Leibson, P. J. (2000). A balance between positive and negative signals in cytotoxic lymphocytes regulates the polarization of lipid rafts during the development of cell-mediated killing. *J. Exp. Med.* **191**, 347-354.

Maasho, K., Opoku-Anane, J., Marusina, A. I., Coligan, J. E. and Borrego, F. (2005). NKG2D is a costimulatory receptor for human naive CD8+ T cells. *J. Immunol.* **174**, 4480-4484.

Mayor, S. and Riezman, H. (2004). Sorting GPI-anchored proteins. *Nat. Rev. Mol. Cell Biol.* **5**, 110-120.

McGilvray, R. W., Eagle, R. A., Watson, N. F., Al-Attar, A., Ball, G., Jafferji, I., Trowsdale, J. and Durrant, L. G. (2009). NKG2D ligand expression in human colorectal cancer reveals associations with prognosis and evidence for immunoediting. *Clin. Cancer Res*. **15**, 6993-7002.

McGilvray, R. W., Eagle, R. A., Rolland, P., Jafferji, I., Trowsdale, J. and Durrant, L. G. (2010). ULBP2 and RAET1E NKG2D ligands are independent predictors of poor prognosis in ovarian cancer patients. *Int. J. Cancer* **127**, 1412-1420.

Mohney, R. P., Knez, J. J., Ravi, L., Sevlever, D., Rosenberry, T. L., Hirose, S. and Medof, M. E. (1994). Glycoinositol phospholipid anchor-defective K562 mutants with biochemical lesions distinct from those in Thy-1- murine lymphoma mutants. *J. Biol. Chem.* **269**, 6536-6542.

Moran, P., Raab, H., Kohr, W. J. and Caras, I. W. (1991). Glycophospholipid membrane anchor attachment. Molecular analysis of the cleavage/attachment site. *J. Biol. Chem.* **266**, 1250-1257.

Nausch, N. and Cerwenka, A. (2008). NKG2D ligands in tumor immunity. *Oncogene* **27**, 5944-5958.

Nociari, M. M., Shalev, A., Benias, P. and Russo, C. (1998). A novel one-step, highly sensitive fluorometric assay to evaluate cell-mediated cytotoxicity. *J. Immunol. Methods* **213**, 157-167.

O'Callaghan, C. A., Cerwenka, A., Willcox, B. E., Lanier, L. L. and Bjorkman, P. J. (2001). Molecular competition for NKG2D: H60 and RAE1 compete unequally for NKG2D with dominance of H60. *Immunity* **15**, 201-211.

Paulick, M. G. and Bertozzi, C. R. (2008). The glycosylphosphatidylinositol anchor: a complex membrane-anchoring structure for proteins. *Biochemistry* **47**, 6991-7000.

Ravetch, J. V. and Perussia, B. (1989). Alternative membrane forms of Fc gamma RIII(CD16) on human natural killer cells and neutrophils. Cell type-specific expression of two genes that differ in single nucleotide substitutions. *J. Exp. Med.* **170**, 481-497.

Sharom, F. J. and Lehto, M. T. (2002). Glycosylphosphatidylinositol-anchored proteins: structure, function, and cleavage by phosphatidylinositol-specific phospholipase C. *Biochem. Cell Biol.* **80**, 535-549.

Stevens, V. L., Zhang, H. and Harreman, M. (1996). Isolation and characterization of a Chinese hamster ovary (CHO) mutant defective in the second step of glycosylphosphatidylinositol biosynthesis. *Biochem. J.* **313**, 253-258.

Suemizu, H., Radosavljevic, M., Kimura, M., Sadahiro, S., Yoshimura, S., Bahram, S. and Inoko, H. (2002). A basolateral sorting motif in the MICA cytoplasmic tail. *Proc. Natl. Acad. Sci. USA* **99**, 2971-2976.

Vales-Gomez, M., Browne, H. and Reyburn, H. T. (2003). Expression of the UL16 glycoprotein of Human Cytomegalovirus protects the virus-infected cell from attack by natural killer cells. *BMC Immunol.* **4**, 4.

Verneris, M. R., Karami, M., Baker, J., Jayaswal, A. and Negrin, R. S. (2004). Role of NKG2D signaling in the cytotoxicity of activated and expanded CD8+ T cells. *Blood* **103**, 3065-3072.

Yu, J., Nagarajan, S., Knez, J. J., Udenfriend, S., Chen, R. and Medof, M. E. (1997). The affected gene underlying the class K glycosylphosphatidylinositol (GPI) surface protein defect codes for the GPI transamidase. *Proc. Natl. Acad. Sci. USA* **94**, 12580-12585.

Journal of Cell Science